Orientation and heat capacity of horizontally adsorbed molecules in electric fields

Ying-Yen Liao*

Department of Applied Physics, National University of Kaohsiung, Kaohsiung 811, Taiwan

(Received 6 June 2013; revised manuscript received 30 January 2014; published 18 February 2014)

The orientation and the heat capacity of horizontally adsorbed molecules are investigated in static electric fields. We evaluate the energy spectrum and the wave function to probe the rotational characteristics of the molecule. Numerical results indicate that the electric field and the effect of quantum confinement lead to anticrossing behaviors in the energy levels. The orientation reveals a stepped feature due to the anticrossing in the ground state. Moreover, the heat capacity displays two peaks near the anticrossing. By means of comparison, each peak of the heat capacity corresponds to a particular degree of orientation.

DOI: 10.1103/PhysRevA.89.022510 PACS number(s): 33.20.Sn, 05.70.−a, 68.43.−h

I. INTRODUCTION

Manipulating molecular rotation has attracted widespread interest for applications such as surface reaction and quantum-information processing [1,2]. The molecules provide an advantage to the controllability via external influences coupling with their dipole moments [3,4]. When the molecule is subject to an electromagnetic field, a hybridization of rotational states is generated to build a specific angular distribution. Such a distribution dynamically reflects the spatial direction of the molecules [5,6]. On the other hand, a static electric field is also able to orient the molecular axis with the help of the interaction between the field and its permanent dipole moment [7]. The stronger field causes the higher degree of orientation. Moreover, the energy levels start to split and shift, depending on the strength of the electric field [8,9].

A number of researched works have been implemented to investigate the rotational behavior of molecules in various systems [10–14]. In these executed systems, the molecules freely rotate without external confinement. Once the molecule is confined, its rotation will become distinguished from one of the free rotors [15,16]. An example is a molecule adsorbed or trapped on a surface [17]. The configurations involving vertical and horizontal adsorption are used to model the molecule-surface system [18–22]. The hindered rotation in the configurations leads to pronounced properties on the energy spectrum, rotational-state distribution, and quadrupole moment [23]. These specific results originate from the interaction between the molecule and its surrounding environment. To probe the rotational properties of adsorbed molecules, various molecular parameters were measured by manipulating electron-energy-loss spectroscopy, neutron scattering, and laser-induced desorption [24–26]. Several kinds of confining potentials are theoretically proposed to address the hindered rotation [27–29]. However, further efforts towards the spatial direction and thermodynamic property of adsorbed molecule are still lacking, especially for orientation and heat capacity. The orientation is different from the heat capacity, yet they are closely associated with the rotational properties such as energy and wave function. To exploit the research, we aim to study the influence of the electric field on the orientation and the heat capacity of horizontally adsorbed molecules. The electric field provides a controllable tool to modify the orientation and the heat capacity of molecules. Both of them are expected to provide rich information about the characteristics of hindered rotation.

In this paper, we investigate the orientation and the heat capacity of horizontally adsorbed molecules in a static electric field. The model of a conical well is proposed to describe the condition of hindered rotation. Numerical results demonstrate that the electric field effectively modifies the energies and the wave functions of molecules. Anticrossing behaviors in the energy levels are clearly observed by tuning the electric field. Specifically, the modified energy states lead to a stepped orientation. The heat capacity exhibits two peaks at low-temperature phases. We further correlate the orientation with the heat capacity. The peak of the heat capacity corresponds to a particular orientation.

This paper is organized as follows. In Sec. II, we describe the conical well model for horizontally adsorbed molecules. In Sec. III, we analyze the results for the energy, wave function, orientation, and heat capacity in detail. In Sec. IV, we give a brief discussion of the results. Finally, there is a conclusive summary at the end.

II. CONICAL WELL MODEL

We consider a system of a polar diatomic molecule that is horizontally adsorbed on a surface. The motion of the adsorbed molecule is subject to a surface potential [18,23]. A conical well is proposed to model the surface potential, as illustrated in Fig. 1. The well is assumed to be independent of azimuthal angle ϕ and is divided into three regions with different potential barriers [28]. When a static electric field along the z axis is externally applied to the configuration of horizontal adsorption, the total Hamiltonian within the rigid-rotor approximation reads

$$H = B\mathbf{J}^2 + V_c - \omega\cos\theta, \tag{1}$$

where $\mathbf{J}$ is the angular momentum operator, B is the rotational constant, and ω is the field-strength parameter, which is equal to $\mu\varepsilon$ for the dipole moment μ and electric field ε. The conical well V_c, which consists of regions I ($0 \leqslant \theta < \alpha$), II ($\alpha \leqslant \theta \leqslant \beta$), and III ($\beta < \theta \leqslant \pi$), is given by

$$V_c(\theta) = \begin{cases} V_0, & 0 \leqslant \theta < \alpha, \\ 0, & \alpha \leqslant \theta \leqslant \beta, \\ V_0, & \beta < \theta \leqslant \pi, \end{cases} \tag{2}$$

*yyliao@nuk.edu.tw

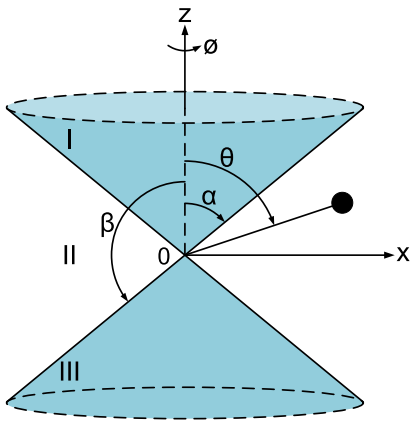

FIG. 1. (Color online) Schematic diagram showing a conical well with hindrance angles α and β. The structure of the well is independent of the azimuthal angle ϕ and is further divided into regions I ($0 \leqslant \theta < \alpha$), II ($\alpha \leqslant \theta \leqslant \beta$), and III ($\beta < \theta \leqslant \pi$). The solid circle indicates the molecular moment of inertia.

where α and β are the hindrance angles and V_0 is the barrier height of the well.

In order to obtain the rotational properties of adsorbed molecules, one can solve the Schrödinger equation of the total Hamiltonian as follows:

$$H\Psi_{\sigma,m} = E_{\sigma,m}\Psi_{\sigma,m}, \tag{3}$$

where $E_{\sigma,m}$ is the energy and $\Psi_{\sigma,m}$ is the wave function for the (σ,m) energy state. The (σ,m) and $(\sigma,-m)$ states are degenerate. The wave function $\Psi_{\sigma,m}$ can be expanded as

$$\Psi_{\sigma,m}(\theta,\phi) = \sum_{l,m} c_{l,m}\psi_{l,m}(\theta,\phi), \tag{4}$$

where $c_{l,m}$ is the expanded coefficient, corresponding to the quantum number (l,m). The basis wave function $\psi_{l,m}$ in Eq. (4) is the eigenfunction of the field-free system, which is described as [23]

$$\psi_{l,m}(\theta,\phi) = \begin{cases} C^{\mathrm{I}}_{l,m} P_{\mathrm{I}}\left(\upsilon^{\mathrm{I}}_{l,m},m,\zeta\right)\exp(im\phi), & \zeta_1 < \zeta \leqslant 1, \\ C^{\mathrm{II}}_{l,m} P_{\mathrm{II}}\left(\upsilon^{\mathrm{II}}_{l,m},m,\zeta\right)\exp(im\phi) + D^{\mathrm{II}}_{l,m} Q_{\mathrm{II}}\left(\upsilon^{\mathrm{II}}_{l,m},m,\zeta\right)\exp(im\phi), & \zeta_2 \leqslant \zeta \leqslant \zeta_1, \\ C^{\mathrm{III}}_{l,m} P_{\mathrm{III}}\left(\upsilon^{\mathrm{III}}_{l,m},m,\zeta\right)\exp(im\phi), & -1 \leqslant \zeta < \zeta_2, \end{cases} \tag{5}$$

with $\zeta = \cos\theta$, $\zeta_1 = \cos\alpha$, and $\zeta_2 = \cos\beta$. Here, the corresponding eigenvalue is determined by $\upsilon^{\mathrm{II}}_{l,m}(\upsilon^{\mathrm{II}}_{l,m}+1)B$. The parameters $\upsilon^{\mathrm{I}}_{l,m}$, $\upsilon^{\mathrm{II}}_{l,m}$, and $\upsilon^{\mathrm{III}}_{l,m}$ are the continuous positive numbers, and $C^{\mathrm{I}}_{l,m}$, $C^{\mathrm{II}}_{l,m}$, $C^{\mathrm{III}}_{l,m}$, and $D^{\mathrm{II}}_{l,m}$ are the normalization constants [28]. The functions P_{I}, P_{II}, P_{III}, and Q_{II} are described as

$$P_{\mathrm{I}}\left(\upsilon^{\mathrm{I}}_{l,m},m,\zeta\right) = (1-\zeta^2)^{|m|/2} F\left(|m| - \upsilon^{\mathrm{I}}_{l,m}, 1+|m|+\upsilon^{\mathrm{I}}_{l,m}, 1+|m|; \frac{1-\zeta}{2}\right), \tag{6}$$

$$P_{\mathrm{II}}\left(\upsilon^{\mathrm{II}}_{l,m},m,\zeta\right) = (1-\zeta^2)^{|m|/2} F\left(|m| - \upsilon^{\mathrm{II}}_{l,m}, 1+|m|+\upsilon^{\mathrm{II}}_{l,m}, 1+|m|; \frac{1-\zeta}{2}\right), \tag{7}$$

$$P_{\mathrm{III}}\left(\upsilon^{\mathrm{III}}_{l,m},m,\zeta\right) = (1-\zeta^2)^{|m|/2} F\left(|m| - \upsilon^{\mathrm{III}}_{l,m}, 1+|m|+\upsilon^{\mathrm{III}}_{l,m}, 1+|m|; \frac{1+\zeta}{2}\right), \tag{8}$$

$$\begin{aligned} Q_{\mathrm{II}}\left(\upsilon^{\mathrm{II}}_{l,m},m,\zeta\right) = (1-\zeta^2)^{|m|/2} \Bigg\{ & F\left(|m| - \upsilon^{\mathrm{II}}_{l,m}, 1+|m|+\upsilon^{\mathrm{II}}_{l,m}, 1+|m|; \frac{1-\zeta}{2}\right) \ln\left(\frac{1-\zeta}{2}\right) \\ & + \sum_{n=1}^{\infty} \frac{\left(|m| - \upsilon^{\mathrm{II}}_{l,m}\right)_n \left(1+|m|+\upsilon^{\mathrm{II}}_{l,m}\right)_n}{(1+|m|)_n n!} \left(\frac{1-\zeta}{2}\right)^n \Big[\psi\left(|m| - \upsilon^{\mathrm{II}}_{l,m} + n\right) - \psi\left(|m| - \upsilon^{\mathrm{II}}_{l,m}\right) \\ & + \psi\left(1+|m|+\upsilon^{\mathrm{II}}_{l,m}+n\right) - \psi\left(1+|m|+\upsilon^{\mathrm{II}}_{l,m}\right) - \psi(1+|m|+n) + \psi(1+|m|) - \psi(1+n) + \psi(1)\Big] \\ & - \sum_{n=1}^{|m|} \frac{(n-1)!(-|m|)_n}{\left(1-|m|+\upsilon^{\mathrm{II}}_{l,m}\right)_n \left(-|m|-\upsilon^{\mathrm{II}}_{l,m}\right)_n} \left(\frac{1-\zeta}{2}\right)^{-n} \Bigg\}, \end{aligned} \tag{9}$$

where ψ is the digamma function and F is the hypergeometric function [30]. To match the boundary conditions at angles α and β, the value of $\upsilon^{\mathrm{II}}_{l,m}$ is numerically determined by the following equation:

$$\begin{aligned} & \left[P_{\mathrm{I}}\left(\upsilon^{\mathrm{I}}_{l,m},m,\zeta_1\right) P'_{\mathrm{II}}\left(\upsilon^{\mathrm{II}}_{l,m},m,\zeta_1\right) - P'_{\mathrm{I}}\left(\upsilon^{\mathrm{I}}_{l,m},m,\zeta_1\right) P_{\mathrm{II}}\left(\upsilon^{\mathrm{II}}_{l,m},m,\zeta_1\right)\right]\left[Q_{\mathrm{II}}\left(\upsilon^{\mathrm{II}}_{l,m},m,\zeta_2\right) P'_{\mathrm{III}}\left(\upsilon^{\mathrm{III}}_{l,m},m,\zeta_2\right)\right. \\ & \left. - Q'_{\mathrm{II}}\left(\upsilon^{\mathrm{II}}_{l,m},m,\zeta_2\right) P_{\mathrm{III}}\left(\upsilon^{\mathrm{III}}_{l,m},m,\zeta_2\right)\right] - \left[P_{\mathrm{I}}\left(\upsilon^{\mathrm{I}}_{l,m},m,\zeta_1\right) Q'_{\mathrm{II}}\left(\upsilon^{\mathrm{II}}_{l,m},m,\zeta_1\right) - P'_{\mathrm{I}}\left(\upsilon^{\mathrm{I}}_{l,m},m,\zeta_1\right) Q_{\mathrm{II}}\left(\upsilon^{\mathrm{II}}_{l,m},m,\zeta_1\right)\right] \\ & \times \left[P_{\mathrm{II}}\left(\upsilon^{\mathrm{II}}_{l,m},m,\zeta_2\right) P'_{\mathrm{III}}\left(\upsilon^{\mathrm{III}}_{l,m},m,\zeta_2\right) - P'_{\mathrm{II}}\left(\upsilon^{\mathrm{II}}_{l,m},m,\zeta_2\right) P_{\mathrm{III}}\left(\upsilon^{\mathrm{III}}_{l,m},m,\zeta_2\right)\right] = 0, \end{aligned} \tag{10}$$

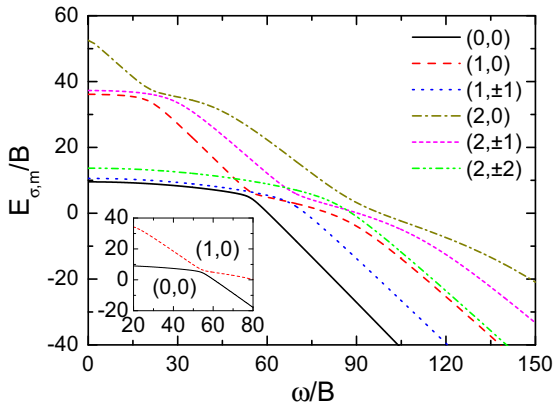

FIG. 2. (Color online) Low-lying energy levels as a function of the field-strength parameter. The inset locally shows the (0,0) and (1,0) states near an anticrossing.

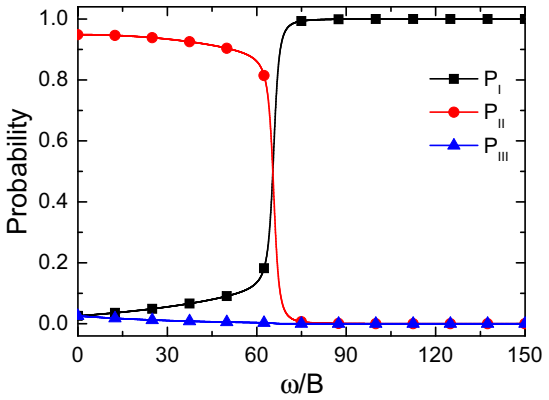

FIG. 3. (Color online) Probabilities of the ground state occurring in regions I, II, and III.

with $\upsilon_{l,m}^{\mathrm{I(III)}}(\upsilon_{l,m}^{\mathrm{I(III)}}+1)B = \upsilon_{l,m}^{\mathrm{II}}(\upsilon_{l,m}^{\mathrm{II}}+1)B - V_0$, $P_{\mathrm{I}}' = dP_{\mathrm{I}}/d\zeta$, $P_{\mathrm{II}}' = dP_{\mathrm{II}}/d\zeta$, $P_{\mathrm{III}}' = dP_{\mathrm{III}}/d\zeta$, and $Q_{\mathrm{II}}' = dQ_{\mathrm{II}}/d\zeta$. Therefore, one can further obtain the orientation and the heat capacity based on the energy and wave function.

III. NUMERICAL RESULTS

To capture the main features of hindered rotation, we consider a symmetric conical well in the work. The parameters $V_0/B = 50$, $\alpha = 70^\circ$, and $\beta = 110^\circ$ are used throughout the calculations. Both effects of the electric field on the rotational energies for $\omega > 0$ and $\omega < 0$ are the same; that is, the energy structure is symmetric with respect to $\omega = 0$. For simplicity, the related properties are only presented in the case of $\omega > 0$. Figure 2 shows the low-lying rotational energies in the electric field. The energy spectrum strongly depends on the strength of the electric field. In the region of weak field, one can find that lower energies are not sensitive to the electric field. The spacings between energy levels approximate to constant values. The result indicates that the hindering potential strongly confines the rotation of the molecule. If the influence of electric field becomes dominant, however, the molecule will overwhelm the confinement of the hindering potential. The energies eventually are diminished with increasing strength. The behavior is similar to that of a free rotor [31]. Specifically, for the ground state, one can observe an anticrossing between the (0,0) and (1,0) states at $\omega^*/B = 54.35$. The corresponding energy spacing at the anticrossing point is 1.82 in units of the rotational constant B. The surrounding region is enlarged in the inset of Fig. 2, where it is clearly seen that both levels repel each other because of the same quantum number m. We can discover similar phenomena for other parts of the spectrum.

The spatial distribution of the wave function is applied to analyze the confinement effect of the well. For the ground state, the probabilities occurring in regions I, II, and III are respectively given by

$$P_{\mathrm{I}} = \int_0^{2\pi}\int_0^{\alpha} |\Psi_{0,0}(\theta,\phi)|^2 \sin\theta d\theta d\phi, \tag{11}$$

$$P_{\mathrm{II}} = \int_0^{2\pi}\int_{\alpha}^{\beta} |\Psi_{0,0}(\theta,\phi)|^2 \sin\theta d\theta d\phi, \tag{12}$$

$$P_{\mathrm{III}} = \int_0^{2\pi}\int_{\beta}^{\pi} |\Psi_{0,0}(\theta,\phi)|^2 \sin\theta d\theta d\phi, \tag{13}$$

with $P_{\mathrm{I}} + P_{\mathrm{II}} + P_{\mathrm{III}} = 1$. The probabilities for the (0,0) state are plotted in Fig. 3. In general, the values smoothly vary in the electric fields. In the weak field, P_{II} is dominant over P_{I} and P_{III}. The ground state mostly locates inside the well (region II). For instance, the value of P_{II} is about 0.93 at $\omega/B = 5$. However, with increasing strength in the field, the rotor will be facilitated to overcome the hindering potential. Then the ground state spreads out of the well, i.e., regions I and III. Probabilities P_{I} and P_{III} become contributive, depending on the direction of the field. For the dominator, P_{I} is 0.99 at $\omega/B = 100$, while P_{III} is 0.99 at $\omega/B = -100$. It is worth mentioning that the probabilities undergo drastic transformations near the anticrossing area. The feature is similarly observed near the anticrossing area at $\omega < 0$. In spite of the two areas, the total probabilities are mainly concentrated in one of the regions. Consequently, by tuning the electric field, one can control the localization and the delocalization of the wave function among the three regions via the anticrossings.

Subsequently, we turn to discuss the effect of the external field on the orientation [32,33]. The orientation of the adsorbed molecule is written as

$$\langle\cos\theta\rangle_T = \frac{1}{Z}\sum_{\sigma,m}\langle\cos\theta\rangle_{\sigma,m}\exp(-E_{\sigma,m}/k_BT), \tag{14}$$

where k_B is the Boltzmann constant, T is the temperature, $\langle\cos\theta\rangle_{\sigma,m}$ stands for the expectation value $\langle\Psi_{\sigma,m}|\cos\theta|\Psi_{\sigma,m}\rangle$, and Z is the partition function denoted by

$$Z = \sum_{\sigma,m}\exp(-E_{\sigma,m}/k_BT). \tag{15}$$

The magnitude of orientation ranges from -1 to 1. Figure 4 shows the field-dependent orientation at low temperature. In the low-temperature region, the low-lying energy states are contributed primarily to the orientation. At $k_BT/B = 0$, the ground state dominates the degree of orientation. The

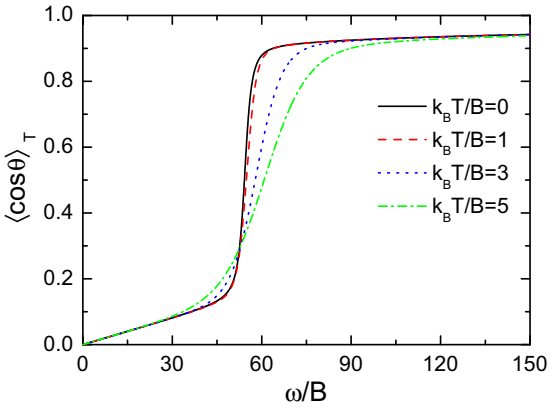

FIG. 4. (Color online) Orientation as a function of the field-strength parameter for different temperatures.

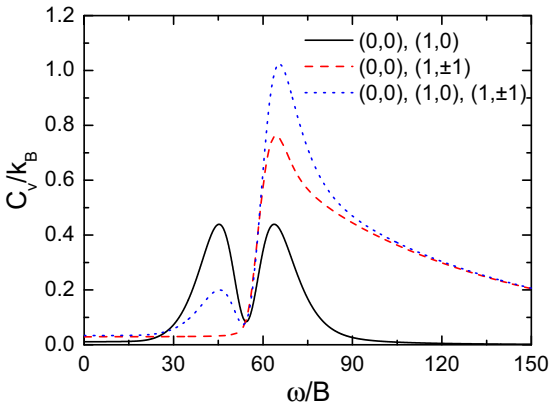

FIG. 6. (Color online) Heat capacity for different contributions of the (0,0), (1,0), and (1, ± 1) states. The temperature is $k_BT/B = 3$.

orientation reveals a stepped feature. For a strong field, the orientation reaches a high value, which is up to 0.93 at $\omega/B = 100$. In this situation, the molecule prefers to orient along the electric field, i.e., the z axis. On the contrary, the orientation becomes small in the case of a weak field. At $\omega/B = 5$, the value of the orientation is 1.3×10^{-2}. This phenomenon implies that the molecule favors a horizontal rotation. It is worth noting that the orientation drastically jumps around the anticrossing region. As the temperature increases, excited energy states increasingly make contributions. The stepped feature gradually becomes less pronounced at higher temperatures.

The heat capacity can be generated from the energy spectrum [34,35]. According to the partition in Eq. (15), the heat capacity of an adsorbed-molecule system is derived by

$$C_V = k_B T \frac{d^2}{dT^2}(T \ln Z). \tag{16}$$

Figure 5 shows the heat capacity at different temperatures. At $k_BT/B = 1$, one can obtain smooth behavior in the case of a weak field. The result is derived from the constant spacings between lower energy levels, as seen in Fig. 2. When ω is tuned around the anticrossing region, the heat capacity obviously manifests the main peak at $k_BT/B = 1$. However, more large

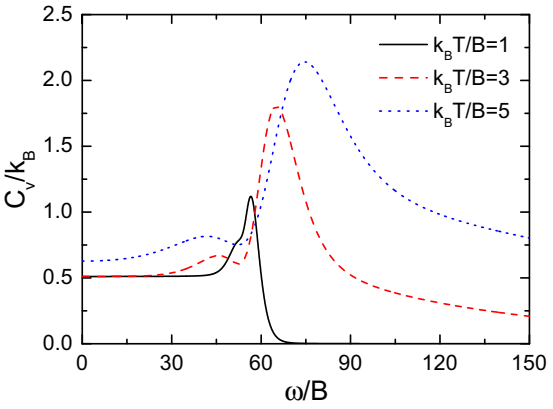

FIG. 5. (Color online) Heat capacity as a function of the field-strength parameter for different temperatures.

spacings between energy levels yield a suppressed behavior in the strong field. As the temperature rises, the peak grows and shifts. In addition, the heat capacity begins to generate a small peak in the proximity of the main one. The ratio of the main to small peaks is 2.7 : 1 at $k_BT/B = 3$. The irregular effect on the peaks results from asymmetric energy levels, as clearly shown in Fig. 2.

In order to analyze the origin of the two-peak feature, the (0,0), (1,0), and (1, ± 1) states are chosen to analyze the heat capacity at low temperature. For the contribution of the (0,0) and (1,0) states, the partition is $Z = \exp(-E_{0,0}/k_BT) + \exp(-E_{1,0}/k_BT)$. The corresponding heat capacity reads

$$C_V = k_B \left(\frac{E_{1,0} - E_{0,0}}{2k_BT}\right)^2 \mathrm{sech}^2\left(\frac{E_{1,0} - E_{0,0}}{2k_BT}\right). \tag{17}$$

As depicted in Fig. 6, the heat capacity reveals the two-peak feature near the anticrossing (black solid line). Furthermore, the drop between two peaks is observed at the anticrossing point $\omega = \omega^*$. To determine the position of the peak, we estimate the maximum of the heat capacity from Eq. (17). According to the equation

$$\tanh\left(\frac{E_{1,0} - E_{0,0}}{2k_BT}\right) - \frac{2k_BT}{E_{1,0} - E_{0,0}} = 0, \tag{18}$$

the peak takes place at the condition of spacing $E_{1,0} - E_{0,0} \simeq 2.4k_BT$. Such a significant phenomenon corresponds to a Schottky anomaly [34]. As shown in Figs. 2 and 6, it is obvious that the unique energy structure results in two Schottky anomalies. Although the same energy spacings lead to the anomalies, the peaks correspond to various distributions of the energy state in the conical well (see Fig. 3). On the contrary, the contribution of the (0,0) and (1, ± 1) states fails to form the two-peak profile (red dashed line). In contrast to the above cases, the more precise value is obtained from the combination of the (0,0), (1,0), and (1, ± 1) states (blue dotted line). As a result, the presence of the anticrossing is crucial to the two-peak feature.

IV. DISCUSSION

The orientation and the heat capacity are obtained from rotational properties of the system. They are different from

quantum ring and dot systems based on the electronic properties [36–39]. The orientation mainly depends on the wave function of the energy state [32,33], whereas the distribution of the wave function determines the degree of orientation. In contrast, the heat capacity depends on the energy levels [34,35]. The level structure affects the behavior of the heat capacity. For the adsorbed-molecule system, the conical well provides the effect of the finite confinement on the rotational properties. The orientation and the heat capacity indeed jointly reflect the consequence. However, if the barrier height V_0 approaches infinity, the strong confinement will lead to the fact that the molecule only rotates inside the conical well [18]. In other words, all of the wave functions localize in region II. The anticrossing behavior will be totally suppressed so that the orientation and the heat capacity do not reveal the related features. In order to concretely explore the configuration of horizontal adsorption, the conical-well model is applied to the system of OH molecules on a Au[111] or Cu[110] surface. We estimate the values of the essential properties by utilizing the given parameters. The rotational constant of OH molecule is 18.91 cm^{-1}, and its dipole moment is 1.6676 D [40,41]. For a conical well, the height is $V_0 = 117.2$ meV. Owing to the confinement effect, the energies of the ground and first excited states are $E_{0,0} = 22.3$ and $E_{1,0} = 84.6$ meV at the zero electric field. The electric field modulates the behaviors of the two states so that the anticrossing point appears at $\varepsilon = 3.6 \times 10^9$ V/m.

We further correlate the orientation with the heat capacity, as shown in Figs. 4 and 5. They can correspond to each other. For example, the heat capacity implies a particular orientation under a given electric field. Specifically, the main peak of heat capacity corresponds to a strong degree of orientation, implying a situation where the adsorbed molecule rotates along the field direction. We take the example of $k_BT/B = 3$. The main peak corresponds to $\langle \cos\theta \rangle_T = 0.78$. Conversely, the small peak denotes a small degree of orientation, where the adsorbed molecule prefers a horizontal rotation. The small peak corresponds to $\langle \cos\theta \rangle_T = 0.15$. Therefore, one can obtain more insight into the adsorbed-molecule system through the connection between the orientation and the heat capacity.

We compare the conical-well model in the configuration of horizontal adsorption with some relevant systems. The one that we take into account is the configuration of vertical adsorption, in which the molecule prefers to be vertically adsorbed on the surface [28]. The rotational motion of the vertically adsorbed molecule is frustrated and different from that of a free rotor. The hindering potential corresponding to such a configuration is a conical-well structure which is described as

$$V_c(\theta) = \begin{cases} 0, & 0 \leqslant \theta \leqslant \alpha, \\ V_0, & \alpha < \theta \leqslant \pi, \end{cases} \tag{19}$$

where α is the hindrance angle and V_0 is the barrier height of the well. Like the potential in Eq. (2), the conical well is independent of azimuthal angle ϕ and is divided into two regions. For the complexity, the potential in Eq. (19) is simpler than that in Eq. (2). Since the electric field is turned on, the vertically adsorbed molecule is pushed to overcome the hindering potential and make only one anticrossing appear in the ground state [16]. The result is distinct from that of the two anticrossings in this model, where the electric field is tuned from $\omega < 0$ to $\omega > 0$. The difference of anticrossing values between the two conical-well models is caused by the structure of the hindering potential. According to the simpler potential in Eq. (19), it is anticipated that the vertically adsorbed molecule shows a one-step orientation, and its behavior is relatively monotone compared to the orientation of the model. For heat capacity, the vertical-adsorption system displays two Schottky anomalies, observed near the anticrossing in the ground state [16]. By contrast, the horizontal-adsorption system reveals four Schottky anomalies due to the two anticrossings in the ground state. In addition to conical-well structures, the periodic potential is proposed to model the hindered rotation [42]. For example, the hindering potential is given by

$$V_c(\phi) = \frac{V_0}{2}(1 + \cos m\phi). \tag{20}$$

The periodic potential has m minima which are divided by m barriers of height V_0. Different from conical-well models, the wave function of the molecule only depends on ϕ. The corresponding Schrödinger equation can be reduced to the Mathieu equation [30,43]. Such a hindered rotation has a pronounced influence on the specific heat in the oxygen-doped germanium and graphite system [29,35]. If the electric field is further applied to the system, the modulated hindered rotation probably leads to interesting behavior in the orientation and related thermodynamic properties.

The adsorbed-molecule system may be extended to interesting applications such as surface reaction and quantum-information processing [1,2]. In general, the relative orientation of reactants plays a crucial role in the chemical reaction. When the reactants collide in the correct orientation spatially, the reaction between them occurs. Otherwise, it gets suppressed in the case of incorrect orientation. As a result, manipulating the orientation becomes significant in the field [11,44]. In this model, the molecule is horizontally adsorbed on the surface. Its rotational motion is confined by the hindering potential. The result demonstrates that the electric field flexibly modulates the degree of orientation. One can manipulate the adsorbed-molecule orientation to effectively control the reaction between a certain reactant and the adsorbed molecule on the surface. Such manipulation may be feasible for a surface reaction. On the other hand, various molecular systems have been investigated for quantum-information processing [2,45]. Entanglement is fundamentally important in the field. A basic scheme consisting of two polar molecules is established to explore its nature [46,47]. The entanglement can be generated via the dipole-dipole interaction. However, these studies are limited in free-rotor systems. On the contrary, a new scheme may be established on the basis of a surface system, where two polar molecules are horizontally adsorbed on the surface. The entanglement arises from the dipole-dipole interaction between the two hindered molecules. As mentioned before, since the electric field modulates the rotational properties of the adsorbed molecule, one can flexibly control the degree of entanglement by tuning the electric field. In addition, the distinctive anticrossing features may lead to interesting properties in entanglement. Consequently, the underlying physics in the conical-well model is useful

for applications in molecular systems based on hindered rotation.

V. CONCLUSIONS

We have investigated the orientation and the heat capacity of horizontally adsorbed molecules in a static electric field. The modified energy states manifest significant phenomena due to the influence of the hindering potential and electric field. The orientation clearly reveals a stepped characteristic at low temperature. Furthermore, the heat capacity exhibits two peaks with different magnitudes. In particular, each peak corresponds to a distinct orientation. The remarkable features of the orientation and heat capacity result from the anticrossing in the ground state.

ACKNOWLEDGMENT

This work is supported by the National Science Council of Taiwan under Grant No. NSC 100-2112-M-390-002-MY3.

[1] D. Shreenivas, A. Lee, N. Walter, D. Sampayo, S. Bennett, and T. Seideman, J. Phys. Chem. A **114**, 5674 (2010).
[2] D. DeMille, Phys. Rev. Lett. **88**, 067901 (2002).
[3] B. Friedrich and D. Herschbach, Phys. Rev. Lett. **74**, 4623 (1995).
[4] D. Townsend, B. J. Sussman, and A. Stolow, J. Phys. Chem. A **115**, 357 (2011).
[5] P. W. Dooley, I. V. Litvinyuk, K. F. Lee, D. M. Rayner, M. Spanner, D. M. Villeneuve, and P. B. Corkum, Phys. Rev. A **68**, 023406 (2003).
[6] M. Machholm and N. E. Henriksen, Phys. Rev. Lett. **87**, 193001 (2001).
[7] J. M. Rost, J. C. Griffin, B. Friedrich, and D. R. Herschbach, Phys. Rev. Lett. **68**, 1299 (1992).
[8] Y. Y. Liao, Phys. Rev. A **85**, 023415 (2012).
[9] S. Y. T. van de Meerakker, H. L. Bethlem, N. Vanhaecke, and G. Meijer, Chem. Rev. **112**, 4828 (2012).
[10] L. Cai, J. Marango, and B. Friedrich, Phys. Rev. Lett. **86**, 775 (2001).
[11] H. Stapelfeldt and T. Seideman, Rev. Mod. Phys. **75**, 543 (2003).
[12] M. Muramatsu, M. Hita, S. Minemoto, and H. Sakai, Phys. Rev. A **79**, 011403(R) (2009).
[13] K. Kitano, N. Ishii, and J. Itatani, Phys. Rev. A **84**, 053408 (2011).
[14] J. J. Omiste and R. González-Férez, Phys. Rev. A **86**, 043437 (2012).
[15] Y. Kohama, T. Rachi, J. Jing, Z. Li, J. Tang, R. Kumashiro, S. Izumisawa, H. Kawaji, T. Atake, H. Sawa, Y. Murata, K. Komatsu, and K. Tanigaki, Phys. Rev. Lett. **103**, 073001 (2009).
[16] Y. Y. Liao, Phys. Rev. B **83**, 115444 (2011).
[17] W. Ho, J. Chem. Phys. **117**, 11033 (2002).
[18] U. Landman, G. G. Kleiman, C. L. Cleveland, E. Kuster, R. N. Barnett, and J. W. Gadzuk, Phys. Rev. B **29**, 4313 (1984).
[19] K. Svensson, L. Bengtsson, J. Bellman, M. Hassel, M. Persson, and S. Andersson, Phys. Rev. Lett. **83**, 124 (1999).
[20] J. W. Riehl and C. J. Fisher, J. Chem. Phys. **59**, 4336 (1973).
[21] R. P. Pan, R. D. Etters, K. Kobashi, and V. Chandrasekharan, J. Chem. Phys. **77**, 1035 (1982).
[22] K. B. K. Tang, R. E. Palmer, D. Teillet-Billy, and J. P. Gauyacq, Chem. Phys. Lett. **277**, 321 (1997).
[23] Y. T. Shih, Y. Y. Liao, and D. S. Chuu, Phys. Rev. B **68**, 075402 (2003).
[24] L. Bengtsson, K. Svensson, M. Hassel, J. Bellman, M. Persson, and S. Andersson, Phys. Rev. B **61**, 16921 (2000).
[25] J. Z. Larese, T. Arnold, L. Frazier, R. J. Hinde, and A. J. Ramirez-Cuesta, Phys. Rev. Lett. **101**, 165302 (2008).
[26] I. Beauport, K. Al-Shamery, and H.-J. Freund, Chem. Phys. Lett. **256**, 641 (1996).
[27] J. W. Gadzuk, U. Landman, E. J. Kuster, C. L. Cleveland, and R. N. Barnett, Phys. Rev. Lett. **49**, 426 (1982).
[28] Y. T. Shih, D. S. Chuu, and W. N. Mei, Phys. Rev. B **54**, 10938 (1996).
[29] H. Shima and T. Nakayama, Phys. Rev. B **71**, 155210 (2005).
[30] *Handbook of Mathematical Functions with Formulas, Graphs and Mathematical Tables*, edited by M. Abramowitz and I. A. Stegun (Dover, New York, 1965).
[31] T. E. Wall, S. K. Tokunaga, E. A. Hinds, and M. R. Tarbutt, Phys. Rev. A **81**, 033414 (2010).
[32] C. M. Dion, A. B. Haj-Yedder, E. Cancès, C. Le Bris, A. Keller, and O. Atabek, Phys. Rev. A **65**, 063408 (2002).
[33] R. Tehini, M. Z. Hoque, O. Faucher, and D. Sugny, Phys. Rev. A **85**, 043423 (2012).
[34] S. Mahdavifar and A. Akbari, J. Phys. Condens. Matter **20**, 215213 (2008).
[35] T. Iwata and M. Watanabe, Phys. Rev. B **81**, 014105 (2010).
[36] A. Matos-Abiague and J. Berakdar, Phys. Rev. B **70**, 195338 (2004).
[37] A. M. Alexeev and M. E. Portnoi, Phys. Rev. B **85**, 245419 (2012).
[38] N. T. T. Nguyen and F. M. Peeters, Phys. Rev. B **78**, 045321 (2008).
[39] B. Boyacioglu and A. Chatterjee, J. Appl. Phys. **112**, 083514 (2012).
[40] A. A. Radzig and B. M. Smirnov, *Reference Data on Atoms, Molecules and Ions* (Springer, Berlin, 1985).
[41] W. L. Meerts and A. Dymanus, Chem. Phys. Lett. **23**, 45 (1973).
[42] W. Forst, *Unimolecular Reactions: A Concise Introduction* (Cambridge University Press, Cambridge, 2003).
[43] M. Leibscher and B. Schmidt, Phys. Rev. A **80**, 012510 (2009).
[44] V. Aquilanti, M. Bartolomei, F. Pirani, D. Cappelletti, F. Vecchiocattivi, Y. Shimizu, and T. Kasai, Phys. Chem. Chem. Phys. **7**, 291 (2005).
[45] K. Mishima and K. Yamashita, J. Chem. Phys. **130**, 034108 (2009).
[46] Q. Wei, S. Kais, B. Friedrich, and D. Herschbach, J. Chem. Phys. **134**, 124107 (2011).
[47] E. Charron, P. Milman, A. Keller, and O. Atabek, Phys. Rev. A **75**, 033414 (2007).